STATUS OF PAPERS

Elizabeth Worcester, for the APB

DUNE Collaboration Call

December 13, 2019

Overview

- APB Procedure Reminders
- Status of DUNE papers
- Details on TDR papers
  - Long-Baseline Sensitivity
  - Supernova Burst Capabilities
  - Beyond the Standard Model Sensitivity

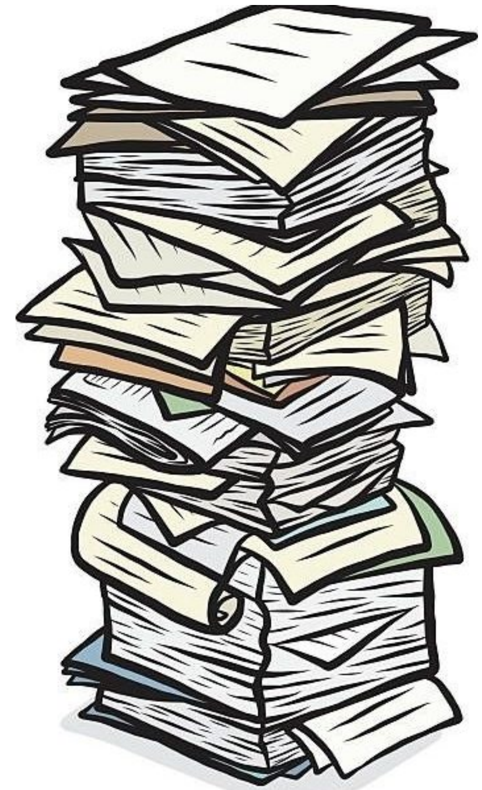

Analysis & Publication Board Reminders

- APB Membership:
  - Chair: Mark Messier
  - Deputy: Frank Filthaut
  - Membership: Mark Convery, Albert de Roeck, Laura Fields, Roxanne Guenette, Ryan Nichol, Thomas Patzak, Ina Sarcevic, Joao Torres, Jeremy Hewes, Ryan Patterson (physics coordinator), Elizabeth Worcester (physics coordinator)
- APB Policy: DocDB 1115
  - Currently exercising these policies for the first time – some details are being filled in by the APB as needed
- General Procedure:
  - Proceedings, technical papers, and physics papers should all go through the APB process!
  - Contact appropriate coordination team (eg: Ryan and Elizabeth for physics papers) early in the process to discuss plans for paper content
  - Notify APB when draft is ready to begin reviews
  - Draft of paper undergoes working group review (minimum 1 week)
  - APB works with paper authors to establish analysis review committee (ARC, ~5 people) for full collaboration papers or coordinator (1 person) for proceedings or technical papers
  - Review by ARC or paper coordinator
  - Presentation of results to full collaboration (collaboration meeting or monthly phone call) for full collaboration papers
  - Collaboration review
  - Journal submission

DUNE Author List

DEEP UNDERGROUND NEUTRINO EXPERIMENT

- Author is defined as “a member of the collaboration working on DUNE for at least a year and having fulfilled an obligation of service work (tasks of general utility to the collaboration other than analysis)” – see publications policy for details
- In November, the APB circulated an author list for the TDR which will serve as the baseline author list for DUNE papers
  - DocDB 16856
  - Opportunity was provided for corrections/additions
  - APB is making their way through the 141 comments that were received (~100 implemented so far)
- Baseline author list will be updated periodically (~every 6 months)
- The APB will consider case-by-case exceptional authors for individual papers – these authors would be added to the author list for a particular paper as a result of a specific contribution to the work presented

Status of Papers

- Technical Papers
  - Neutrino-electron elastic scattering for flux determination at the DUNE oscillation experiment -- submitted
  - 35T TPC – collaboration review
  - A measurement of absolute efficiency of the ARAPUCA photon detector in Liquid Argon – collaboration review
  - The Effects of Thermal Cycling on Two Light Guide 2 Technologies and Two Readout Technologies in Liquid – collaboration review
  - The protoDUNE-SP LArTPC Electronics Production, Commissioning, and Performance – coordinator assigned
- DUNE Physics Papers
  - TDR: Long-Baseline Sensitivity – ARC chair identified, committee forming
  - TDR: Supernova Burst Capabilities – ARC chair identified, committee forming
  - TDR: Beyond the Standard Model Sensitivity – working group review starting soon
  - Neutrino Interaction Classification with the DUNE Convolutional Visual Network – ARC chair identified, committee forming
  - protoDUNE Single Phase – draft in progress (see next talk)

TDR Papers

- Three papers specifically based on TDR physics volume text planned:
  - Long-Baseline Sensitivity
  - Supernova Burst Capabilities
  - Beyond the Standard Model Sensitivity
- Content drawn from the TDR, with some reduction in details
  - Focus on the physics analyses
  - Remove content added for review purposes (pedagogy, gory details, etc)
  - Does not preclude future publications with more detail or improved studies
- Papers targeting EPJC
  - Spokes and PCs have been in contact with a journal editor
- Status and contacts
  - Mature drafts exist for all three papers
  - LBL paper:
    - Working group contact: Callum Wilkinson
    - ARC Chair: Morgan Wascko
  - SNB paper:
    - Working group contact: Kate Scholberg
    - ARC Chair: Bryce Littlejohn
  - BSM paper:
    - Working group contacts: Lisa Koerner, Alex Sousa, Jae Yu
    - ARC coming soon

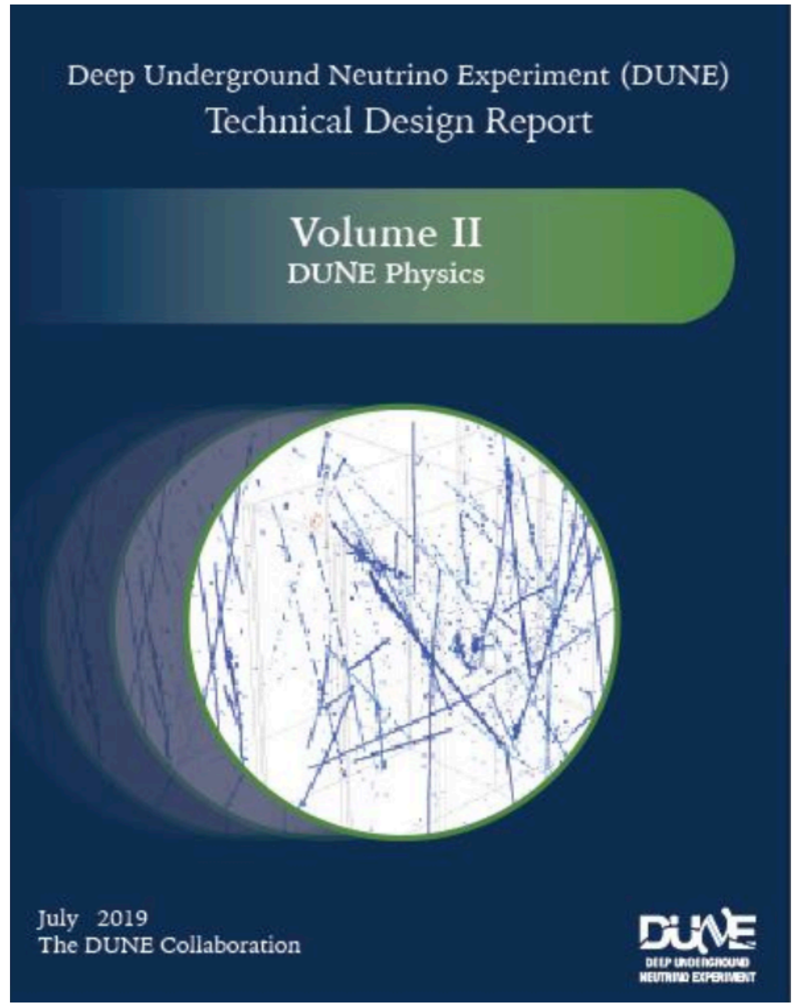

Note on Procedures for TDR Papers

- Because the analyses presented in these papers are identical to the TDR analyses, the results have already been fully vetted by the collaboration and the LBNC. The charge for the ARCs and collaboration review is to comment on the effectiveness with which the papers present the analyses.
- For the same reason, in the interest of time, we consider the step of presenting the analysis to the collaboration in advance of collaboration review to be already fulfilled.
- Expect to distribute the papers for collaboration comments before the January collaboration meeting

“Long-baseline neutrino oscillation physics potential of the DUNE experiment”

DEEP UNDERGROUND NEUTRINO EXPERIMENT

- 25 pages in 2-column format, 25 figures, 11 tables

12

to missing energy in unreconstructed final-state neutrinos. The selected NC and CC ν_μ generally include an asymmetric decay of a relatively high energy π^0 coupled with a prompt photon conversion. As can be seen in Figure 11, the background to the ν_μ disappearance are due to wrong-sign ν_μ interactions, which cannot be easily distinguished in the unmagnetized DUNE FD, and NC interactions, where a pion has been misidentified as the muon. As expected, the ν_μ background in RHC is much larger than the $\bar{\nu}_\mu$ background in FHC.

Sample	Expected Events (3.5 years staged)
ν mode	
ν_e Signal NO (IO)	1092 (497)
$\bar{\nu}_e$ Signal NO (IO)	18 (31)
Total Signal NO (IO)	1110 (528)
Beam $\nu_e + \bar{\nu}_e$ CC background	190
NC background	81
$\nu_\tau + \bar{\nu}_\tau$ CC background	32
$\nu_\mu + \bar{\nu}_\mu$ CC background	14
Total background	317
$\bar{\nu}$ mode	
ν_e Signal NO (IO)	76 (36)
$\bar{\nu}_e$ Signal NO (IO)	224 (470)
Total Signal NO (IO)	300 (506)
Beam $\nu_e + \bar{\nu}_e$ CC background	117
NC background	38
$\nu_\tau + \bar{\nu}_\tau$ CC background	20
$\nu_\mu + \bar{\nu}_\mu$ CC background	5
Total background	180

TABLE VI: ν_e and $\bar{\nu}_e$ appearance rates: integrated rate of selected ν_e CC-like events between 0.5 and 8.0 GeV assuming a 3.5-year (staged) exposure in the neutrino-beam mode and antineutrino-beam mode. The signal rates are shown for both normal mass ordering (NO) and inverted mass ordering (IO), and all the background rates assume normal mass ordering. All the rates assume $\delta_{CP} = 0$.

VII. DETECTOR UNCERTAINTIES

Detector effects impact the event selection efficiency as well as the reconstruction of quantities used in the oscillation fit, such as neutrino energy. The main sources of detector systematic uncertainties are limitations of the expected calibration and modeling of particles in the detector.

Sample	Expected Events (3.5 years staged)
ν mode	
ν_μ Signal	6200
$\bar{\nu}_\mu$ CC background	389
NC background	200
$\nu_\tau + \bar{\nu}_\tau$ CC background	46
$\nu_e + \bar{\nu}_e$ CC background	8
$\bar{\nu}$ mode	
$\bar{\nu}_\mu$ Signal	2303
ν_μ CC background	1129
NC background	101
$\nu_\tau + \bar{\nu}_\tau$ CC background	27
$\nu_e + \bar{\nu}_e$ CC background	2

TABLE VII: ν_μ and $\bar{\nu}_\mu$ disappearance rates: integrated rate of selected ν_μ CC-like events between 0.5 and 8.0 GeV assuming a 3.5-year (staged) exposure in the neutrino-beam mode and antineutrino-beam mode. The rates are shown for normal mass ordering and $\delta_{CP} = 0$.

Parameter	Central value	Relative uncertainty
θ_{12}	0.5903	2.3%
θ_{23} (NO)	0.866	4.1%
θ_{23} (IO)	0.869	4.0%
θ_{13} (NO)	0.150	1.5%
θ_{13} (IO)	0.151	1.5%
Δm^2_{21}	7.39×10^{-5} eV^2	2.8%
Δm^2_{32} (NO)	2.451×10^{-3} eV^2	1.3%
Δm^2_{32} (IO)	-2.512×10^{-3} eV^2	1.3%
ρ	2.848 g cm^{-3}	2%

TABLE VIII: Central value and relative uncertainty of neutrino oscillation parameters from a global fit [5, 47] to neutrino oscillation data. The matter density is taken from Ref. [48]. Because the probability distributions are somewhat non-Gaussian (particularly for θ_{23}), the relative uncertainty is computed using 1/6 of the 3σ allowed range from the fit, rather than the 1σ range. For θ_{23}, θ_{13}, and Δm^2_{31}, the best-fit values and uncertainties depend on whether normal mass ordering (NO) or inverted mass ordering (IO) is assumed.

13

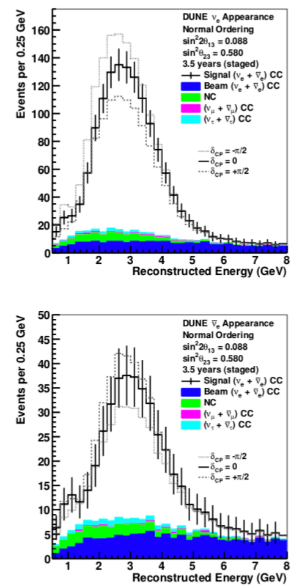

FIG. 10: ν_e and $\bar{\nu}_e$ appearance spectra: reconstructed energy distribution of selected ν_e CC-like events assuming 3.5 years (staged) running in the neutrino-beam mode (top) and antineutrino-beam mode (bottom), for a total of seven years (staged) exposure. The plots assume normal mass ordering and include curves for $\delta_{CP} = -\pi/2, 0$, and $\pi/2$.

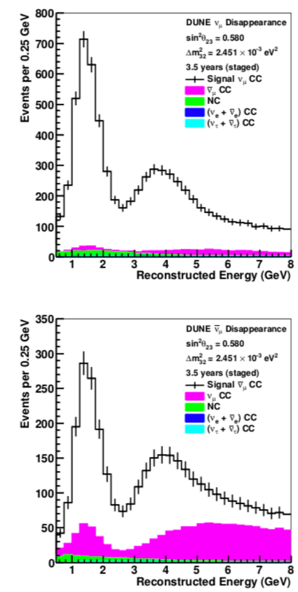

FIG. 11: ν_μ and $\bar{\nu}_\mu$ disappearance spectra: reconstructed energy distribution of selected ν_μ CC-like events assuming 3.5 years (staged) running in the neutrino-beam mode (top) and antineutrino-beam mode (bottom), for a total of seven years (staged) exposure. The plots assume normal mass ordering.

The ND LArTPC uses similar technology to the FD, but important differences lead to uncertainties that do not fully correlate between the two detectors. First, the readout technology is different, as the near LArTPC uses pixels as well as a different, modular photon detector. Therefore, the charge response will be different between near and far due to differences in electronics readout, noise, and local effects like alignment. Second, the high-intensity environment of the ND complicates associating detached energy deposits to events, a problem which does not exist in the FD. Third, the calibration programs will be different. For example, the ND has a high-statistics calibration sample of through-going, momentum-analyzed muons from neutrino interactions in the upstream rock, which does not exist for the FD.

LBL Content

- Outline:
  - Introduction (1.5 pages)
  - Flux and uncertainties (1.5 pages)
  - Neutrino interactions and uncertainties (2 pages)
  - Near detector sim/reco (2.5 pages)
  - Far detector sim/reco (2.5 pages)
  - Far detector event rate and oscillation parameters (2.5 pages)
  - Detector uncertainties (2 pages)
  - Sensitivity methods (1.5 pages)
  - Sensitivities (5 pages)
  - Conclusion (0.5 pages)
- Major changes with respect to LBL TDR chapter
  - Remove much of the pedagogical introductory material
  - Add some figures and discussion from the "Tools and Methods" TDR chapter regarding simulation and reconstruction
  - Remove some of the detailed discussion of interaction physics, focusing more on what was done for this analysis
  - Remove a few less-interesting sensitivity plots
  - Remove discussion of event samples from ND that were not included in this analysis and section on impact of near detector (save for a later paper)

“Supernova Neutrino Burst Detection with the Deep Underground Neutrino Experiment”

- 19 pages in 2-column format, 15 figures, 1 table

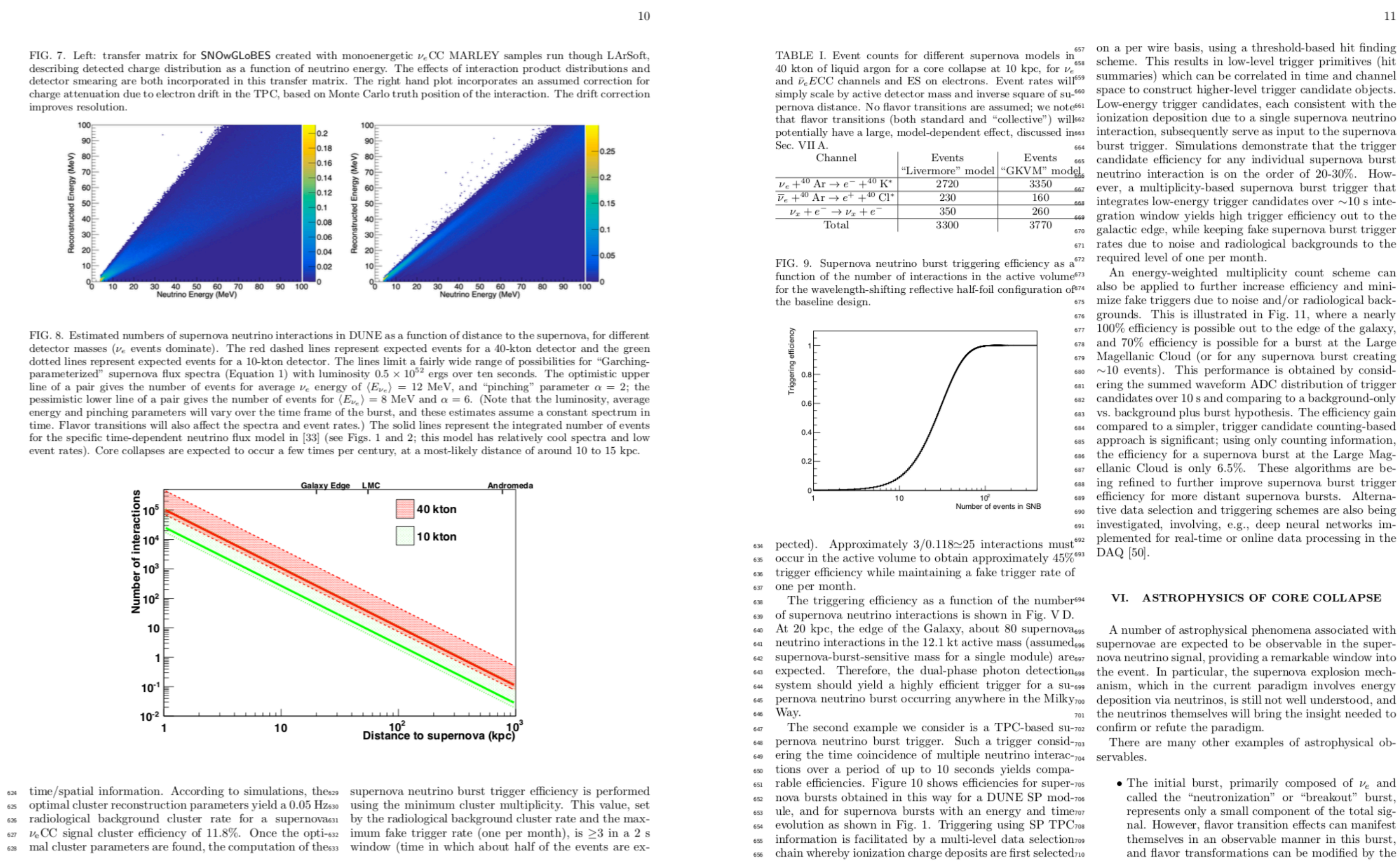

FIG. 7. Left: transfer matrix for SNOwGLoBES created with monoenergetic ν_eCC MARLEY samples run though LArSoft, describing detected charge distribution as a function of neutrino energy. The effects of interaction product distributions and detector smearing are both incorporated in this transfer matrix. The right hand plot incorporates an assumed correction for charge attenuation due to electron drift in the TPC, based on Monte Carlo truth position of the interaction. The drift correction improves resolution.

FIG. 8. Estimated numbers of supernova neutrino interactions in DUNE as a function of distance to the supernova, for different detector masses (ν_e events dominate). The red dashed lines represent expected events for a 40-kton detector and the green dotted lines represent expected events for a 10-kton detector. The lines limit a fairly wide range of possibilities for “Garching-parameterized” supernova flux spectra (Equation 1) with luminosity 0.5×10^{52} ergs over ten seconds. The optimistic upper line of a pair gives the number of events for average ν_e energy of $\langle E_{\nu_e} \rangle = 12$ MeV, and “pinching” parameter $\alpha = 2$; the pessimistic lower line of a pair gives the number of events for $\langle E_{\nu_e} \rangle = 8$ MeV and $\alpha = 6$. (Note that the luminosity, average energy and pinching parameters will vary over the time frame of the burst, and these estimates assume a constant spectrum in time. Flavor transitions will also affect the spectra and event rates.) The solid lines represent the integrated number of events for the specific time-dependent neutrino flux model in [33] (see Figs. 1 and 2; this model has relatively cool spectra and low event rates). Core collapses are expected to occur a few times per century, at a most-likely distance of around 10 to 15 kpc.

time/spatial information. According to simulations, the optimal cluster reconstruction parameters yield a 0.05 Hz radiological background cluster rate for a supernova ν_eCC signal cluster efficiency of 11.8%. Once the optimal cluster parameters are found, the computation of the supernova neutrino burst trigger efficiency is performed using the minimum cluster multiplicity. This value, set by the radiological background cluster rate and the maximum fake trigger rate (one per month), is ≥3 in a 2 s window (time in which about half of the events are ex-

TABLE I. Event counts for different supernova models in 40 kton of liquid argon for a core collapse at 10 kpc, for ν_e and $\bar{\nu}_e E$CC channels and ES on electrons. Event rates will simply scale by active detector mass and inverse square of supernova distance. No flavor transitions are assumed; we note that flavor transitions (both standard and “collective”) will potentially have a large, model-dependent effect, discussed in Sec. VII A.

Channel	Events “Livermore” model	Events “GKVM” model
$\nu_e + {}^{40}\mathrm{Ar} \to e^- + {}^{40}\mathrm{K}^*$	2720	3350
$\overline{\nu}_e + {}^{40}\mathrm{Ar} \to e^+ + {}^{40}\mathrm{Cl}^*$	230	160
$\nu_x + e^- \to \nu_x + e^-$	350	260
Total	3300	3770

FIG. 9. Supernova neutrino burst triggering efficiency as a function of the number of interactions in the active volume for the wavelength-shifting reflective half-foil configuration of the baseline design.

pected). Approximately 3/0.118≃25 interactions must occur in the active volume to obtain approximately 45% trigger efficiency while maintaining a fake trigger rate of one per month.

The triggering efficiency as a function of the number of supernova neutrino interactions is shown in Fig. V D. At 20 kpc, the edge of the Galaxy, about 80 supernova neutrino interactions in the 12.1 kt active mass (assumed supernova-burst-sensitive mass for a single module) are expected. Therefore, the dual-phase photon detection system should yield a highly efficient trigger for a supernova neutrino burst occurring anywhere in the Milky Way.

The second example we consider is a TPC-based supernova neutrino burst trigger. Such a trigger considering the time coincidence of multiple neutrino interactions over a period of up to 10 seconds yields comparable efficiencies. Figure 10 shows efficiencies for supernova bursts obtained in this way for a DUNE SP module, and for supernova bursts with an energy and time evolution as shown in Fig. 1. Triggering using SP TPC information is facilitated by a multi-level data selection chain whereby ionization charge deposits are first selected on a per wire basis, using a threshold-based hit finding scheme. This results in low-level trigger primitives (hit summaries) which can be correlated in time and channel space to construct higher-level trigger candidate objects. Low-energy trigger candidates, each consistent with the ionization deposition due to a single supernova neutrino interaction, subsequently serve as input to the supernova burst trigger. Simulations demonstrate that the trigger candidate efficiency for any individual supernova burst neutrino interaction is on the order of 20-30%. However, a multiplicity-based supernova burst trigger that integrates low-energy trigger candidates over ∼10 s integration window yields high trigger efficiency out to the galactic edge, while keeping fake supernova burst trigger rates due to noise and radiological backgrounds to the required level of one per month.

An energy-weighted multiplicity count scheme can also be applied to further increase efficiency and minimize fake triggers due to noise and/or radiological backgrounds. This is illustrated in Fig. 11, where a nearly 100% efficiency is possible out to the edge of the galaxy, and 70% efficiency is possible for a burst at the Large Magellanic Cloud (or for any supernova burst creating ∼10 events). This performance is obtained by considering the summed waveform ADC distribution of trigger candidates over 10 s and comparing to a background-only vs. background plus burst hypothesis. The efficiency gain compared to a simpler, trigger candidate counting-based approach is significant; using only counting information, the efficiency for a supernova burst at the Large Magellanic Cloud is only 6.5%. These algorithms are being refined to further improve supernova burst trigger efficiency for more distant supernova bursts. Alternative data selection and triggering schemes are also being investigated, involving, e.g., deep neural networks implemented for real-time or online data processing in the DAQ [50].

VI. ASTROPHYSICS OF CORE COLLAPSE

A number of astrophysical phenomena associated with supernovae are expected to be observable in the supernova neutrino signal, providing a remarkable window into the event. In particular, the supernova explosion mechanism, which in the current paradigm involves energy deposition via neutrinos, is still not well understood, and the neutrinos themselves will bring the insight needed to confirm or refute the paradigm.

There are many other examples of astrophysical observables.

- The initial burst, primarily composed of ν_e and called the “neutronization” or “breakout” burst, represents only a small component of the total signal. However, flavor transition effects can manifest themselves in an observable manner in this burst, and flavor transformations can be modified by the

SNB Content

- Outline
  - Introduction (0.5 pages)
  - The Supernova Burst Neutrino Landscape (1.5 pages)
    - Current experiments, experiments in DUNE era, beyond core-collapse
  - Supernova Neutrino Bursts (1 page)
  - The DUNE Detector (0.5 pages)
  - Low-Energy Events in DUNE (6.5 pages)
    - Detection Channels and Interaction Rates, Event Simulation and Reconstruction, Expected SNB Signal, Triggering
  - Astrophysics of Core Collapse (3 pages)
  - Neutrino Physics and Other Particle Physics (2 pages)
  - Conclusion (<0.5 pages)
- Major changes with respect to the TDR chapter
  - Significant restructuring
  - Addition of information on triggering and DAQ taken from the detector volume
  - Remove most discussion of solar neutrinos (mentioned briefly, save for later paper)
  - Remove discussion of SNB pointing (save for later paper)

“Physics Beyond the Standard Model at DUNE”

DEEP UNDERGROUND NEUTRINO EXPERIMENT

- 41 pages in 2-column format (32 pages excluding citations), 39 figures, 9 tables

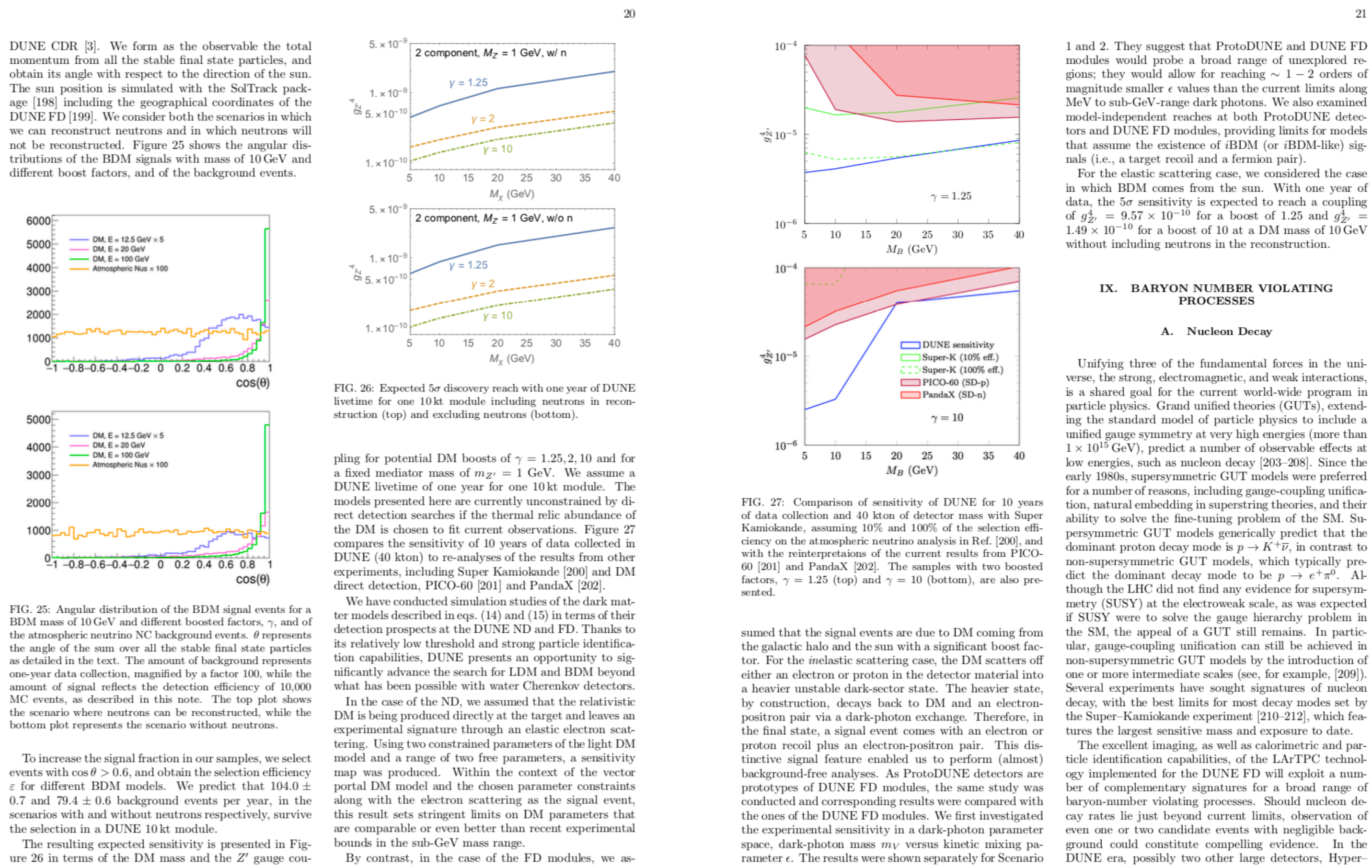

20

DUNE CDR [3]. We form as the observable the total momentum from all the stable final state particles, and obtain its angle with respect to the direction of the sun. The sun position is simulated with the SolTrack package [198] including the geographical coordinates of the DUNE FD [199]. We consider both the scenarios in which we can reconstruct neutrons and in which neutrons will not be reconstructed. Figure 25 shows the angular distributions of the BDM signals with mass of 10 GeV and different boost factors, and of the background events.

FIG. 25: Angular distribution of the BDM signal events for a BDM mass of 10 GeV and different boosted factors, γ, and of the atmospheric neutrino NC background events. θ represents the angle of the sum over all the stable final state particles as detailed in the text. The amount of background represents one-year data collection, magnified by a factor 100, while the amount of signal reflects the detection efficiency of 10,000 MC events, as described in this note. The top plot shows the scenario where neutrons can be reconstructed, while the bottom plot represents the scenario without neutrons.

To increase the signal fraction in our samples, we select events with $\cos\theta > 0.6$, and obtain the selection efficiency ε for different BDM models. We predict that 104.0 ± 0.7 and 79.4 ± 0.6 background events per year, in the scenarios with and without neutrons respectively, survive the selection in a DUNE 10 kt module.

The resulting expected sensitivity is presented in Figure 26 in terms of the DM mass and the Z' gauge coupling for potential DM boosts of $\gamma = 1.25, 2, 10$ and for a fixed mediator mass of $m_{Z'} = 1$ GeV. We assume a DUNE livetime of one year for one 10 kt module. The models presented here are currently unconstrained by direct detection searches if the thermal relic abundance of the DM is chosen to fit current observations. Figure 27 compares the sensitivity of 10 years of data collected in DUNE (40 kton) to re-analyses of the results from other experiments, including Super Kamiokande [200] and DM direct detection, PICO-60 [201] and PandaX [202].

FIG. 26: Expected 5σ discovery reach with one year of DUNE livetime for one 10 kt module including neutrons in reconstruction (top) and excluding neutrons (bottom).

We have conducted simulation studies of the dark matter models described in eqs. (14) and (15) in terms of their detection prospects at the DUNE ND and FD. Thanks to its relatively low threshold and strong particle identification capabilities, DUNE presents an opportunity to significantly advance the search for LDM and BDM beyond what has been possible with water Cherenkov detectors.

In the case of the ND, we assumed that the relativistic DM is being produced directly at the target and leaves an experimental signature through an elastic electron scattering. Using two constrained parameters of the light DM model and a range of two free parameters, a sensitivity map was produced. Within the context of the vector portal DM model and the chosen parameter constraints along with the electron scattering as the signal event, this result sets stringent limits on DM parameters that are comparable or even better than recent experimental bounds in the sub-GeV mass range.

By contrast, in the case of the FD modules, we assumed that the signal events are due to DM coming from the galactic halo and the sun with a significant boost factor. For the *in*elastic scattering case, the DM scatters off either an electron or proton in the detector material into a heavier unstable dark-sector state. The heavier state, by construction, decays back to DM and an electron-positron pair via a dark-photon exchange. Therefore, in the final state, a signal event comes with an electron or proton recoil plus an electron-positron pair. This distinctive signal feature enabled us to perform (almost) background-free analyses. As ProtoDUNE detectors are prototypes of DUNE FD modules, the same study was conducted and corresponding results were compared with the ones of the DUNE FD modules. We first investigated the experimental sensitivity in a dark-photon parameter space, dark-photon mass m_V versus kinetic mixing parameter ϵ. The results were shown separately for Scenario

FIG. 27: Comparison of sensitivity of DUNE for 10 years of data collection and 40 kton of detector mass with Super Kamiokande, assuming 10% and 100% of the selection efficiency on the atmospheric neutrino analysis in Ref. [200], and with the reinterpretaions of the current results from PICO-60 [201] and PandaX [202]. The samples with two boosted factors, $\gamma = 1.25$ (top) and $\gamma = 10$ (bottom), are also presented.

21

1 and 2. They suggest that ProtoDUNE and DUNE FD modules would probe a broad range of unexplored regions; they would allow for reaching $\sim 1-2$ orders of magnitude smaller ϵ values than the current limits along MeV to sub-GeV-range dark photons. We also examined model-independent reaches at both ProtoDUNE detectors and DUNE FD modules, providing limits for models that assume the existence of *i*BDM (or *i*BDM-like) signals (i.e., a target recoil and a fermion pair).

For the elastic scattering case, we considered the case in which BDM comes from the sun. With one year of data, the 5σ sensitivity is expected to reach a coupling of $g^4_{Z'} = 9.57 \times 10^{-10}$ for a boost of 1.25 and $g^4_{Z'} = 1.49 \times 10^{-10}$ for a boost of 10 at a DM mass of 10 GeV without including neutrons in the reconstruction.

IX. BARYON NUMBER VIOLATING PROCESSES

A. Nucleon Decay

Unifying three of the fundamental forces in the universe, the strong, electromagnetic, and weak interactions, is a shared goal for the current world-wide program in particle physics. Grand unified theories (GUTs), extending the standard model of particle physics to include a unified gauge symmetry at very high energies (more than 1×10^{15} GeV), predict a number of observable effects at low energies, such as nucleon decay [203–208]. Since the early 1980s, supersymmetric GUT models were preferred for a number of reasons, including gauge-coupling unification, natural embedding in superstring theories, and their ability to solve the fine-tuning problem of the SM. Supersymmetric GUT models generically predict that the dominant proton decay mode is $p \to K^+\overline{\nu}$, in contrast to non-supersymmetric GUT models, which typically predict the dominant decay mode to be $p \to e^+\pi^0$. Although the LHC did not find any evidence for supersymmetry (SUSY) at the electroweak scale, as was expected if SUSY were to solve the gauge hierarchy problem in the SM, the appeal of a GUT still remains. In particular, gauge-coupling unification can still be achieved in non-supersymmetric GUT models by the introduction of one or more intermediate scales (see, for example, [209]). Several experiments have sought signatures of nucleon decay, with the best limits for most decay modes set by the Super–Kamiokande experiment [210–212], which features the largest sensitive mass and exposure to date.

The excellent imaging, as well as calorimetric and particle identification capabilities, of the LArTPC technology implemented for the DUNE FD will exploit a number of complementary signatures for a broad range of baryon-number violating processes. Should nucleon decay rates lie just beyond current limits, observation of even one or two candidate events with negligible background could constitute compelling evidence. In the DUNE era, possibly two other large detectors, Hyper–

BSM Content

- Outline:
  - Introduction (0.5 pages)
  - Analysis Details (1 page)
  - Sterile Neutrino Mixing (3 pages)
  - Non-Unitarity of the Neutrino Mixing Matrix (1.5 pages)
  - Non-Standard Neutrino Interactions (1.5 pages)
  - CPT Symmetry Violation (3 pages)
  - Neutrino Tridents at the Near Detector (2.5 pages)
  - Dark Matter Probes (7.5 pages)
    - Low-Mass Dark Matter at the ND, Inelastic Boosted Dark Matter at the FD, Elastic Boosted Dark Matter from the Sun
  - Baryon Number Violating Processes (8.5 pages)
    - Nucleon decay, Neutron-antineutron Oscillation
  - Other Physics Opportunities (3 pages)
  - Conclusion (<0.5 pages)
- Major changes with respect to the TDR chapters
  - Restructuring to combine the two relevant chapters
  - No major changes to BSM chapter content
  - Addition of more discussion on impact of FSI on reconstruction and event selection to nucleon decay section
  - Note: no particular significance to order of topics

Conclusion

- DUNE collaborators should be aware of the publication procedures and keep appropriate coordinators and the APB in the loop throughout planning of all papers
  - Includes technical/small-author-list papers and proceedings as well as physics papers
- We are keeping the APB very busy!
  - Huge thank you to Mark, Frank, and the APB members
  - Thank you to everyone serving as a working group contact, paper coordinator, ARC chair, or ARC member
- First full DUNE papers coming soon!
  - Please participate in the collaboration review